Published in final edited form as:
Arch Neurol. 2010 April ; 67(4): 440–446. doi:10.1001/archneurol.2010.34.

Comparable Results of FDG-PET CMR_{glc} and DTBZ-PET K_1 in Evaluation of Early Dementia and Mild Cognitive Impairment

Roger L. Albin, MD, **Robert A. Koeppe, PhD**, **James F. Burke, MD**, **Bruno Giordani, PhD**, **Michael R. Kilbourn, PhD**, **Sid Gilman, MD**, and **Kirk A. Frey, MD, PhD**
VA Ann Arbor Health System Geriatrics Research, Education, and Clinical Center (Dr. Albin); Dept. of Neurology, University of Michigan (Drs. Albin, Burke, Gilman, and Frey); Division of Nuclear Medicine, Dept. of Radiology, University of Michigan (Drs. Koeppe, Kilbourn, and Frey); Dept. of Psychiatry, University of Michigan (Dr. Giordani)

Abstract

Objective—To compare assessment of regional cerebral metabolic changes with DTBZ-PET measurement of regional cerebral blood flow (K_1) and FDG-PET measurement of regional cerebral glucose uptake (CMR_{glc}) in a clinically representative sample of mild dementia and mild cognitive impairment (MCI) subjects. We hypothesized that DTBZ-PET K_1 and FDG-PET CMR_{glc} provide equivalent information.

Design, Setting, Participants—DTBZ-PET K_1 measurement of regional cerebral blood flow and FDG-PET CMR_{glc} measurement of regional cerebral glucose uptake was performed in 50 subjects with either mild dementia (MMSE ≥ 18) or MCI drawn from a university based Cognitive Disorders Clinic. Results were compared with 80 normal control subjects.

Main Outcome Measures—DTBZ-PET regional K_1 measurements and FDG-PET CMR_{glc} measurements were compared with standard correlation analysis. The overall patterns of DTBZ-PET K_1 deficits and FDG-PET CMR_{glc} deficits were assessed with stereotaxic surface projections (SSP) of parametric images.

Results—DTBZ-PET regional K_1 measurements and FDG-PET CMR_{glc} measurements were highly correlated, both within and between subjects. SSP maps of deficits in DTBZ-PET regional K_1 measurements and FDG-PET CMR_{glc}s were markedly similar. DTBZ-PET K_1 SSP maps exhibited a mild decrease in sensitivity relative to FDG-PET CMR_{glc} maps.

Conclusion—DTBZ-PET K_1 and FDG-PET CMR_{glc} provide comparable information in assessment of regional cerebral metabolic deficits in mild dementia and MCI. K_1 measures can assess regional cerebral metabolism deficits accurately in mild dementia and MCI. K_1 assessments of regional cerebral metabolic deficits can be combined with tracer binding results to improve of utility of PET imaging in mild dementia and MCI.

Corresponding Author: Roger L. Albin, MD; 5023 BSRB, 109 Zina Pitcher Place, Ann Arbor, MI, 48109-2200; tel 734-764-1347; fax 734-763-7686; ralbin@umich.edu.

Author Contributions: Dr. Albin had full access to all the data in the study and takes full responsibility for data integrity and data analysis. *Study concept and design:* Albin & Frey. *Acquisition of data:* Albin, Frey, Giordani, Koeppe, Kilbourn. *Analysis and interpretation of data:* Albin, Frey, Koeppe, Giordani, Burke. *Drafting of the manuscript:* Albin & Koeppe. *Critical revision of the manuscript for important intellectual content:* Albin, Koeppe, Burke, Giordani, Kilbourn, Gilman, Frey. *Statistical analysis:* Koeppe. *Obtained funding:* Albin, Frey, & Gilman. *Administrative, technical, and material support:* Koeppe & Kilbourn. *Study supervision:* Albin & Frey.

Financial Disclosure: None reported.

Introduction

The present approach to diagnosis of dementia relies on clinical characterization, psychometric evaluation, and application of standardized clinical criteria[1]. There is overlap in clinical criteria for the three major forms of degenerative dementia - Alzheimer disease (AD), Lewy Body dementia (DLB), and Frontotemporal dementias (FTDs) – and clinical diagnosis has relatively poor specificity[1,2,3,4,5]. Differentiation is particularly difficult in individuals with early, mild dementia. Positron emission tomography (PET) is a useful technique for evaluation of dementias. [^{18}F]Fluoro-deoxyglucose PET (FDG-PET) assessment of regional cerebral metabolic rate for glucose (CMR_{glc}) is the most widely studied PET method for evaluation of dementias[6,7,8]. FDG-PET is useful in determining whether individuals have an underlying cerebral problem, differentiating types of dementia, identifying cerebral abnormalities in individuals with mild cognitive impairment (MCI), predicting the likelihood of progression from MCI, and predicting the rate of progression of dementia[9-28]. FDG-PET identifies characteristic patterns of regional cerebral metabolic changes in AD, DLB, FTDs, and vascular dementia (VaD)[29-39].

PET methods identifying characteristic pathologic features of dementias are being explored. Diminished dopaminergic nigrostriatal terminals are a feature of DLB[40,41]. Single site studies and a recent multicenter clinical trial indicate that PET or single photon emission computed tomography methods measuring nigrostriatal dopaminergic terminal density are useful in establishing a diagnosis of DLB[42,43,44]. Tracers binding to characteristic histopathologic features of dementias, such as the amyloid ligand 2-(4′methylaminophenyl) benzothiazole (BTA-1; Pittsburgh B [PiB]), may provide an *in vivo* analogue of histopathologic diagnosis[45-54]. Determining patterns of altered regional cerebral metabolism and abnormal retention of tracers aimed at characteristic pathologic features should provide complementary information. This can be accomplished by studying patients with FDG-PET and a second PET study using one of the nigrostriatal dopaminergic terminal ligands or [^{11}C]PiB[55]. This approach requires at least 2 scans with accompanying increased expense, radiation exposure, and demands on patients.

Regional cerebral metabolism and regional cerebral blood flow are tightly coupled[56,57,58]. Data analysis for some PET tracers allows determination of the regional cerebral tracer blood to brain transport rate (K_1) as a measure of regional cerebral blood flow. We reported previously that assessment of regional cerebral K_1 of the dopaminergic terminal ligand [^{11}C]dihydrotetrabenazine (DTBZ) produced results closely comparable to measurement of CMR_{glc} with FDG-PET[59]. Our prior study was a retrospective analysis of subjects drawn from a well characterized research cohort not representative of clinical practice. These subjects had moderate AD (mean MMSE score =15), DLB (mean MMSE score = 17, and FTD (mean MMSE score = 23), not the early, mild dementia/MCI subjects in whom accurate clinical diagnosis is most difficult. To confirm the utility of K_1 assessments, we report comparison of FDG-PET assessment of CMR_{glc} with measurements of [^{11}C]DTBZ-PET K_1s in a prospective series of representative subjects undergoing initial characterization of mild dementia and MCI.

Methods

Subjects

Fifty subjects were recruited through the Michigan Alzheimer Disease Research Center as part of an ongoing project studying utility of PET imaging in early dementia and MCI. Subjects are drawn from the Cognitive Disorders Clinic at the University of Michigan. Subjects are excluded if their Mini-Mental State Score (MMSE) was lower than 18 or if they had a confounding neurologic or psychiatric disorder that prevented establishment of a clear

diagnosis of dementia or MCI. Subjects were excluded also if clinical evaluation (including routine structural imaging) indicated a diagnosis of VaD. While this is not a population based cohort, subjects enrolled for this study are representative of patients seen for initial evaluation in tertiary referral cognitive disorders clinics. There is no overlap in subjects between those enrolled in this study and our prior study of DTBZ K_1 and FDG-PET CMR_{glc}.

All subjects underwent standardized clinical and psychometric evaluations. Clinical evaluations consisted of a history and standard neurologic examination performed by a neurologist experienced in the evaluation of dementias. All subjects underwent evaluation for treatable causes of dementia with recommended serum and structural imaging studies[1]. Psychometric evaluation included the Alzheimer Disease Research Center Unified Data Set measures (Digit Span, Category Fluency, Trails Test, Digit Symbol, Wechsler Memory Scale Revised Logical Memory Story A, Boston Naming Test-30-item, Geriatric Depression Scale, Neuropsychiatric Inventory Questionnaire) plus additional standard measures of memory, executive function, attention, language, visuospatial function, mood, and anxiety. Clinical and psychometric data were abstracted into a standard form stripped of identifiers by one of the authors (JFB). Standardized data forms were reviewed in a consensus conference by three authors (RLA, KAF, BG) to assign a consensus diagnosis. Standard criteria were used to assign diagnoses of AD, DLB, and FTD[60,61,62]. For diagnosis of MCI, standard clinical and psychometric criteria were applied[63]. Subjects with MCI were classified as single domain MCI (amnestic or non-amnestic; aMCI or naMCI) or multi-domain MCI (mdMCI). All subjects underwent PET imaging within 3 months of initial evaluation. Scans of 80 age matched, normal subjects studied previously in our center were used as control data (Supplementary Table 1 at http://sitemaker.umich.edu/albinsuppldata). PET Imaging: All subjects underwent [^{11}C]DTBZ and [^{18}F]FDG PET either in the same imaging session or on consecutive days if they were not able to tolerate the 4-hr procedure. DTBZ scans were performed on a Siemens ECAT Exact HR+ scanner (Knoxville, TN), while FDG scans were performed on a Siemens BioGraph Classic PET/CT scanner (Knoxville, TN). Subjects were positioned supine and awake in a quiet dimly lit room with eyes open. For [^{11}C]DTBZ, 666 ± 66 MBq (18 ± 1.8 mCi) of [^{11}C]DTBZ were administered intravenously. An equilibrium protocol was used, infusing 55% of the dose over 30 s, followed by continuous infusion of the remaining 45% over 60 min[64]. [^{18}F]FDG studies were performed as a single 20-min scan acquired 30 min after intravenous injection of 296 ± 29 MBq (8.0 ± 0.8 mCi) of [^{18}F]FDG. All scans were acquired in 3-dimensional (3D) mode. Measured attenuation correction was performed using a 5-min 2-dimensional (2D) transmission scan followed by segmentation and reprojection. Scatter correction was performed on all scans. After Fourier rebinning (FORE) of the 3D projection sinograms into 2D datasets, images were reconstructed using ordered-subset expectation-maximization (OSEM), with 4 iterations and 16 subsets with no additional smoothing, providing both in-plane and axial image resolution of ~5.5 mm full-width at half-maximum.

Image Processing and Data Analysis

The single 20-min [^{18}]FDG image acquired starting 30-min post-injection provided an index of CMR_{glc}. For the [^{11}C]DTBZ scan, the average of the first 4 min of uptake provided our index of ligand transport, K_1. PET images for both measures for each subject were reoriented to a common coordinate system based on the stereotactic atlas of Talairach and Tournoux[65]. After reorientation, all images underwent linear scaling and nonlinear warping[66]. A single transformation based on the individual's summed [^{18}F]FDG and [^{11}C]DTBZ K_1 images was calculated for each subject and then applied to both image sets.

All transaxial levels of the Talairach and Tournoux atlas have been digitized, and a set of standardized cortical and subcortical volumes of interest (VOIs) defined on the atlas

images[59]. A subset of 34 cortical VOIs (17 per hemisphere) was selected for analysis and applied automatically to all images for all mild dementia and MCI subjects, and the 15 control subjects use for correlation analysis of DTBZ K_1 and FDG CMR_{glc}. This set of regions included cortical areas hypothesized to provide the best differentiation between groups. We expected frontal regions, particularly medial, to be affected more in FTD than AD or DLB and posterior parietal/posterior cingulate regions to be more affected in AD and DLB than FTD. We expected the occipital region to be more affected in DLB than AD or FTD, and the region that best differentiates DLB from AD. Sensorimotor cortex was included as a cortical region likely to be affected least in these dementias. FDG and DTBZ K_1 images were normalized to the mean VOI value obtained from the pons and cerebellar vermis[67]. These two regions were selected as the normalizing factor because they are structures known to be minimally involved in these disorders, enhancing the ability to detect regional cortical deficits by removal of the more variable global factor in these measures.

Statistical Analysis

Both within-subject and across-subject correlations were performed. Within-subject correlations were calculated for each of the 50 patient subjects and 15 controls who received both FDG and DTBZ scans. VOI FDG CMR_{glc} and DTBZ K_1 normalized values were correlated for all 34 selected cortical regions. Across-subject correlations were calculated for each of the 34 regions separately for each of the 50 patient and 15 control subjects.

SSP

The use of stereotactic surface projections (SSP) is a standard method for processing FDG CMR_{glc} data to produce easily interpretable parametric images[68]. In this voxel-based method, gray matter activity is projected to the cortical surface in an anatomically standardized manner. The resulting map of brain activity is compared with a database of appropriate matched subjects to generate a Z-score map of deviations from normal. The Z-score maps permit ready visual interpretation of CMR_{glc} deficit patterns. We utilized the Neurostat program and a control database of the 27 FDG controls to generate Z-score maps of FDG CMR_{glc} deficits for all subjects. The SSP approach was used also for processing of DTBZ K_1 images. We constructed a control database from 68 subjects of similar age without clinical evidence of any neurologic disease. These 68 individuals were studied previously in our center using the same scan protocol used in this project.

Results

Subjects

50 subjects with dementia or MCI participated. Mean age was 70 years (SD 10; range 51-91; 28 female; 22 male). There were 19 AD, 5 DLB, and 9 FTD. Sixteen subjects were classified as MCI with 9 aMCI, 4 naMCI, and 3 mdMCI. One subject refused psychometric evaluation and is classified as indeterminate. Of the 80 control subjects scanned, 27 received FDG (mean age 71, SD 9, range 55-88; 13 female, 14 male), and 68 received DTBZ (mean age 68, SD 8, range 55-86, 38 Female, 37 Male). Fifteen control subjects received both FDG and DTBZ scans (mean age 70, SD 9, range 55-86, 8 Female, 7 Male).

FDG CMRglc and DTBZ K1 Correlation Analysis

There was excellent correspondence between regional cerebral metabolism assessed with FDG and regional cerebral blood flow assessed with DTBZ K_1. Regional deficits averaged across all patient subjects, reported as percent of normal control mean, were similar for the two PET measures in most regions examined (Figure 1). Frontal cortical regions did exhibit slightly greater deficits in FDG than in DTBZ K1, reaching significance both laterally and

medially. In other regions, both the magnitude of the declines and the variability across patients were comparable. Individual within-subject correlations between normalized FDG and DTBZ K_1 (across the regions examined; left and right hemisphere for the 17 regions shown in Fig. 2) averaged 0.88±0.07 for the 50 patient subjects (range 0.73-0.96; Figure 2). Within-subject correlations for controls were lower due to the smaller range of values, averaging 0.78±0.08 (range 0.64-0.88). Besides the similarity in image pattern between the measures, the magnitude of the deficits correlated highly. Within-subject correlations of the Z-scores relative to controls average 0.74±0.14 (range 0.37-0.96; Supplementary Figure 1 at http://sitemaker.umich.edu/albinsuppldata). Z-score correlations for controls averaged 0.54±0.25 (range 0.05-0.82). The much broader range of Z-score correlations is due to the nature of the Z-score measure. Control as well as patient subjects who have image patterns similar to the normal mean pattern will have low correlations due to the limited range of data values.

Across-subjects correlations between FDG and DTBZ K_1 varied considerably across the regions examined. Correlations across the 34 regions average 0.78±0.14 (range 0.51-0.94) in patients and 0.76±0.13 (range 0.48-0.91) in controls. Correlations across the patient subjects were uniformly high ($r>0.83$) in cortical regions that show deficits in these patient groups (parietal, frontal cortex, posterior cingulate), while correlations in regions not primarily involved in disease (subcortical structures) were typically much lower. Correlations for a highly affected region, parietal cortex, are seen in Figure 3.

SSP Analysis

SSP analysis was applied to FDG CMR_{glc} and DTBZ K_1 images for each subject as described above. The resulting Z-score maps were compared for qualitative similarity. FDG and DTBZ K_1 Z-score maps were similar for all patients, regardless of diagnosis (Figure 4). In general, DTBZ K_1 Z-score maps tended to identify a smaller number of abnormal surface map pixels. This is due primarily to the slightly higher noise at the pixel level of DTBZ K_1 image than FDG images. For all surface pixels, the coefficient of variation of DTBZ K_1 control subjects averaged 10.4% and that of FDG was 9.6%. In all cases, however, DTBZ K_1 Z-score maps were readily identifiable as abnormal and qualitatively identical to FDG-PET CMR_{glc} Z-score maps. The number of surface map pixels found to be abnormal (more than 2.5 standard deviations below the normal mean) in the most affected regions was higher for FDG than DTBZ K_1 (Figure 5). The total of surface map pixels in the most affected areas (posterior cingulate, lateral parietal, lateral temporal, lateral and medial frontal) was 8920 (Supplementary Figure 2 at http://sitemaker.umich.edu/albinsuppldata). In the most severe patients, over the half the surface pixels have z-scores deficits of greater than 2.5. The regression line of DTBZ K_1 on FDG shows a slope less than unity (0.863) indicating fewer significant pixels for DTBZ. Many of the pixels found to be significant in FDG but not DTBZ K_1 are located in frontal cortex.

Comment

Our results indicate similar properties of FDG-PET assessment of CMRglc and DTBZ-PET K_1 assessment of regional cerebral blood flow to identify regional cerebral metabolic deficits in subjects with MCI and early, mild dementia. Regional cerebral metabolic deficits are characteristic of dementias and specific patterns of deficits are associated with each major form of degenerative dementia[6-15,29-32,33-37]. We did find that DTBZ K_1 assessments tended to be somewhat less sensitive in SSP analysis because of higher variation in surface pixel values. This was most noticeable in frontal regions. This could reduce sensitivity of DTBZ K_1 assessments in FTDs and related disorders.

Differentiation of dementias, based on clinical criteria and using structural imaging and laboratory studies to exclude other causes of dementia, has relatively poor specificity[1]. FDG-PET is suggested to improve diagnosis of dementias and may be cost effective in evaluation of patients with early, mild dementia[69,70,71]. Recent work demonstrates that FDG-PET with SSP analysis differentiates early dementia and controls in a clinically representative population of early dementia and MCI[72]. The "gold standard" for diagnosis of dementias remains histopathologic evaluation. Small series with FDG-PET evaluations followed by histopathologic analysis indicate that FDG-PET evaluation significantly improves specificity without sacrificing sensitivity[8,9,31,73]. These results are consistent with studies in which FDG-PET results were compared with systematic, longitudinal clinical evaluations[69]. Differentiation of dementias at initial evaluation is particularly difficult. Jagust et al. found that initial clinical evaluation of a series of mildly demented patients who were followed to autopsy had relatively poor sensitivity (76%) and specificity (56%) for diagnosis of pathologically confirmed AD, and that diagnostic precision improved significantly with addition of FDG-PET imaging data. Diagnostic sensitivity and specificity of FDG-PET evaluation was comparable to clinical evaluation after several years of followup.

While characteristic metabolic deficits occur in many individuals with dementia, confounding features can reduce accuracy of FDG-PET. There is considerable overlap between AD and DLB. Not all DLB subjects exhibit the typical visual cortex abnormalities; the sensitivity and specificity of FDG-PET for differentiating AD and DLB are not significantly better than application of clinical criteria[32,74]. Pathologic studies indicate that a high percentage of individuals with focal cortical syndromes typical of FTDs exhibit AD pathology[75]. These AD focal cortical syndromes are likely to be classified as FTDs by both clinical criteria and FDG-PET criteria[76,77]. PET tracers aimed at characteristic pathologic features of dementias are likely to be useful in overcoming the limitations of FDG-PET. PET and SPECT ligands identifying the characteristic nigrostriatal dopaminergic deficit of DLB improve differentiation of AD and DLB. Similarly, [^{11}C]PIB is likely to be useful in identifying dementias characterized by substantial Aβ amyloid deposition such as AD and cases of DLB with substantial fibrillary amyloid burden.

Ligand binding results and assessment of regional cerebral metabolic deficits may be complementary. DTBZ-PET studies, for example, could identify nigrostriatal dopaminergic deficits in both DLB and some cases of FTDs[78]. The pattern of regional cerebral metabolic deficits would be useful in differentiating these different syndromes. [^{11}C]DTBZ itself is not likely to become a clinically used ligand but fluorinated DTBZ analogues or another tracer quantifying nigrostriatal terminal density may become available for clinical use. Obtaining both ligand binding and regional cerebral metabolic deficit data from a single PET study will be advantageous in terms of cost, safety, and patient convenience. PET ligands with high brain to blood extraction fractions yield K_1 parametric image data comparable to that obtained with FDG-PET and K_1 parametric image data can be represented as SSP maps. Use of K_1 parametric image data from PET ligands aimed at characteristic pathologic features of dementias is likely to enhance the clinical utility of PET methods for characterization of MCI and early, mild dementias.

Supplementary Material

Refer to Web version on PubMed Central for supplementary material.

Acknowledgments

Funding/Support: Supported by AG08671 & NS15655. The sponsors had no role in data collection, analysis, interpretation, or manuscript preparation.

References

1. Knopman DS, DeKosky ST, Cummings JL, et al. Practice parameter: diagnosis of dementia (an evidence-based review). Neurology. 2001; 56:1143–1153. [PubMed: 11342678]
2. McKeith IG, Ballard CG, Perry RH, Ince PG, O'Brien JT, Neill D, et al. Prospective validation of consensus criteria for the diagnosis of dementia with Lewy bodies. Neurology. 2000; 54:1050–1058. [PubMed: 10720273]
3. Lopez OL, Litvan I, Catt KE, Stowe R, Klunk W, Kaufer DI, et al. Accuracy of four clinical diagnostic criteria for the diagnosis of neurodegenerative dementias. Neurology. 1999; 53:1292–1299. [PubMed: 10522887]
4. Varma AR, Snowden JS, Lloyd JJ, Talbot PR, Mann DM, Neary D. Evaluation of the NINCDS-ADRDA criteria in the differentiation of Alzheimer's disease and frontotemporal dementia. J Neurol Neurosurg Psychiatr. 1999; 66:184–188. [PubMed: 10071097]
5. Rosen HJ, Hartikainen KM, Jagust W, Kramer JH, Reed BR, Cummings JL, et al. Utility of clinical criteria in differentiating frontotemporal lobar degeneration (FTLD) from AD. Neurology. 2002; 58:1608–1615. [PubMed: 12058087]
6. Herholz K, Carter SF, Jones M. Positron emission tomography imaging in dementia. Br J Radiol. 2007:S160–S167. [PubMed: 18445746]
7. Silverman DHS, Mosconi L, Ercoli L, Chen W, Small GW. Positron emission tomography scans obtained for the evaluation of cognitive dysfunction. Sem Nuc Med. 2008; 38:251–261.
8. Mosconi L. Brain glucose metabolism in the early and specific diagnosis of Alzheimer's disease. Eur J Nuc Med. 2005; 32:486–510.
9. Silverman DHS, Small GW, Chang CY, et al. Positron emission tomography in evaluation of dementia: regional brain metabolism and long-term outcome. JAMA. 2001; 286:2120–2127. [PubMed: 11694153]
10. de Leon MJ, Ferris SH, George A, Reisberg B, Christman DR, Kricheff II, et al. Computed tomography and positron emission transaxial tomography evaluations of normal aging and Alzheimer's disease. J Cereb Blood Flow Metab. 1983; 3:391–394. [PubMed: 6603463]
11. Foster NL, Chase TN, Mansi L, Brooks R, Fedio P, Patronas NJ, et al. Cortical abnormalities in Alzheimer's disease. Ann Neurol. 1984; 16:649–654. [PubMed: 6335378]
12. Friedland RP, Brun A, Budinger TF. Pathological and positron emission tomographic correlations in Alzheimer's disease. Lancet. 1985; 26:228. [PubMed: 2857310]
13. Koss E, Friedland RP, Ober BA, Jagust WJ. Differences in lateral hemispheric asymmetries of glucose utilization between early- and late-onset Alzheimer-type dementia. Am J Psychiatr. 1985; 142:638–660. [PubMed: 3872604]
14. Minoshima S, Giordani B, Berent S, Frey KA, Foster NL, Kuhl DE. Metabolic reduction in the posterior cingulate cortex in very early Alzheimer's disease. Ann Neurol. 1997; 42:85–94. [PubMed: 9225689]
15. Herholz K, Salmon E, Perani D, Baron JC, Holthoff V, Frolich L, et al. Discrimination between Alzheimer dementia and controls by automated analysis of multicenter FDG PET. Neuroimage. 2002; 17:302–316. [PubMed: 12482085]
16. Alexander GE, Chen K, Pietrini P, Rapoport SI, Reiman EM. Longitudinal PET evaluation of cerebral metabolic decline in dementia: a potential outcome measure in Alzheimer's disease treatment studies. Am J Psychiatr. 2002; 159:738–745. [PubMed: 11986126]
17. Small GW, Ercoli LM, Silverman DHS, Huang SC, Komo S, Bookheimer S, et al. Cerebral metabolic and cognitive decline in persons at genetic risk for Alzheimer's disease. Proc Natl Acad Sci USA. 2000; 97:6037–6042. [PubMed: 10811879]
18. Reiman EM, Caselli RJ, Chen K, Alexander GE, Bandy D, Frost J. Declining brain activity in cognitively normal apolipoprotein E epsilon 4 heterozygotes: a foundation for using positron

emission tomography to efficiently test treatments to prevent Alzheimer's disease. Proc Natl Acad Sci USA. 2001; 98:3334–3339. [PubMed: 11248079]

19. Reiman EM, Chen K, Alexander GE, Caselli RJ, Bandy D, Osborne D, et al. Functional brain abnormalities in young adults at genetic risk for late-onset Alzheimer's dementia. Proc Natl Acad Sci U S A. 2004; 101:284–9. [PubMed: 14688411]
20. Reiman EM, Caselli RJ, Yun LS, Chen K, Bandy D, Minoshima S, Thibodeau SN, Osborne D. Preclinical evidence of Alzheimer's disease in persons homozygous for the epsilon 4 allele for apolipoprotein E. N Engl J Med. 1996 Mar 21; 334(12):752–8. [PubMed: 8592548]
21. Chetelat G, Desgranges B, De La Sayette V, Viader F, Eustache F, Baron JC. Mild cognitive impairment: can FDG-PET predict who is to rapidly convert to Alzheimer's disease? Neurology. 2003; 60:1374–7. [PubMed: 12707450]
22. Nestor PJ, Fryer TD, Smielewski P, Hodges JR. Limbic hypometabolism in Alzheimer's disease and mild cognitive impairment. Ann Neurol. 2003; 54:343–51. [PubMed: 12953266]
23. Minoshima S, Giordani B, Berent S, Frey KA, Foster NL, Kuhl DE. Metabolic reduction in the posterior cingulate cortex in very early Alzheimer's disease. Ann Neurol. 1997; 42:85–94. [PubMed: 9225689]
24. Arnaiz E, Jelic V, Almkvist O, Wahlund L-O, Winblad B, Valind S, et al. Impaired cerebral glucose metabolism and cognitive functioning predict deterioration in mild cognitive impairment. Neuroreport. 2001; 12:851–5. [PubMed: 11277595]
25. Chetelat G, Desgranges B, De La Sayette V, Viader F, Eustache F, Baron JC. Mild cognitive impairment: can FDG-PET predict who is to rapidly convert to Alzheimer's disease? Neurology. 2003; 60:1374–7. [PubMed: 12707450]
26. Drzezga A, Lautenschlager N, Siebner H, Riemenschneider M, Willoch F, Minoshima S, et al. Cerebral metabolic changes accompanying conversion of mild cognitive impairment into Alzheimer's disease: a PET follow-up study. Eur J Nucl Med Mol Imaging. 2003; 30:1104–13. [PubMed: 12764551]
27. Mosconi L, Sorbi S, Nacmias B, De Cristofaro MTR, Fayyazz M, Cellini E, et al. Brain metabolic differences between sporadic and familial Alzheimer's disease. Neurol. 2003; 61:1138–40.
28. Herholz K, Nordberg A, Salmon E, et al. Impairment of neocortical metabolism predicts progression to Alzheimer's disease. Dement Geriatr Cogn Disord. 1999; 10:494–504. [PubMed: 10559566]
29. Herholz K. PET studies in dementia. Ann Nuc Med. 2003; 17:79–89.
30. Albin RL, Minoshima S, D'Amato C, Frey KA, Kuhl DE, Sima AAF. Fluoro-Deoxyglucose Positron Emission Tomography in Diffuse Lewy Body Disease. Neurology. 1995; 47:462–466. [PubMed: 8757021]
31. Minoshima S, Foster NL, Sima AAF, Frey KA, Albin RL, Kuhl DE. Alzheimer's disease versus dementia with Lewy bodies: cerebral metabolic distinction with autopsy confirmation. Ann Neurol. 2001; 50:358–365. [PubMed: 11558792]
32. Higuchi M, Tashiro M, Arai H, et al. Glucose hypometabolism and neuropathological correlates in brains of dementia with Lewy bodies. Exp Neurol. 2000; 162:247–256. [PubMed: 10739631]
33. Salmon E, Garraux G, Delbueck X, et al. Predominant ventromedial frontopolar metabolic impairment in frontotemporal dementia. NeuroImage. 2003; 20:435–440. [PubMed: 14527604]
34. Diehl-Schmid J, Grimmer T, Drzezga A, et al. Decline of glucose cerebral metabolism in frontotemporal dementia: a longitudinal 18F-FDG-PET-study. Neurobiol Aging. 2007; 28:42–50. [PubMed: 16448722]
35. Foster NL, Heidebrink JL, Clark CM, et al. FDG-PET improve accuracy in distinguishing frontotemporal dementia and Alzheimer's disease. Brain. 2007; 130:2616–2635. [PubMed: 17704526]
36. Ishii K, Sakamoto S, Sasaki M, et al. Cerebral glucose metabolism in patients with frontotemporal dementia. J Nucl Med. 1998; 39:1875–73. [PubMed: 9829574]
37. Jeong Y, Cho SS, Park JM, et al. ^{18}F-FDG PET findings in frontotemporal dementia: an SPM analysis of 29 patients. J Nucl Med. 2005; 46:233–239. [PubMed: 15695781]

38. Tullberg M, Fletcher E, DeCarli C, Mungas D, Reed BR, Harvey DJ, Weiner MW, Chui HC, Jagust WJ. White matter lesions impair frontal lobe function regardless of their location. Neurology. 2004; 63:246–253. [PubMed: 15277616]
39. Kerrouche N, Herholz K, Mielke R, Holthoff V, Baron JC. ^{18}FDG PET in vascular dementia: differentiation from Alzheimer's disease using voxel-based multivariate analysis. J Cereb Blood Flow Metab. 2006; 26:1213–1221. [PubMed: 16525414]
40. Piggott MA, Marshall EF, Thomas N, et al. Striatal dopaminergic markers in dementia with Lewy bodies, Alzheimer's and Parkinson's diseases: rostrocaudal distribution. Brain. 1999; 122:1449–1468. [PubMed: 10430831]
41. Suzuki, Desmond TJ, Albin RL, Frey KA. Striatal monoaminergic terminals in Lewy body dementia and Alzheimer disease. Ann Neurol. 2002; 51:767–771. [PubMed: 12112084]
42. Walker, Costa DC, Walker RWH, et al. Differentiation of dementia with Lewy bodies from Alzheimer's disease using a dopaminergic presynaptic ligand. J Neurol Neurosurg Psychiatry. 2002; 73:134–140. [PubMed: 12122169]
43. Gilman S, Koeppe RA, Little R, et al. Striatal monoaminergic terminals in Lewy body dementia and Alzheimer's disease. Ann Neurol. 2002; 55:774–780. [PubMed: 15174011]
44. McKeith I, O'Brien J, Walker Z, Tatsch K, Booij J, Darcourt J, Padovani A, Giubbini R, Bonuccelli U, Volterrani D, Holmes C, Kemp P, Tabet N, Meyer I, Reininger C. DLB Study Group. Sensitivity and specificity of dopamine transporter imaging with 123I-FP-CIT SPECT in dementia with Lewy bodies: a phase III, multicentre study. Lancet Neurol. 2007; 6:305–313. [PubMed: 17362834]
45. Klunk WE, Engler H, Nordberg A, Wang Y, Blomqvist G, Holt DP, Bergström M, Savitcheva I, Huang GF, Estrada S, Ausén B, Debnath ML, Barletta J, Price JC, Sandell J, Lopresti BJ, Wall A, Koivisto P, Antoni G, Mathis CA, Långström B. Imaging brain amyloid in Alzheimer's disease with Pittsburgh Compound-B. Ann Neurol. 2004; 55:306–319. [PubMed: 14991808]
46. Villemagne VL, Fodero-Tavoletti MT, Pike KE, et al. The ART of loss: Aβ imaging in the evaluation of Alzheimer's disease and other dementias. Mol Neurobiol. 2008; 38:1–15. [PubMed: 18690556]
47. Verhoeff NP, Wilson AA, Takeshita S, Trop L, Hussey D, Singh K, Kung HF, Kung MP, Houle S. In-vivo imaging of Alzheimer disease beta-amyloid with [11C]SB-13 PET. Am J Geriatr Psychiatry. 2004; 12:584–595. [PubMed: 15545326]
48. Rowe CC, Ng S, Ackermann U, Gong SJ, Pike K, Savage G, Cowie TF, Dickinson KL, Maruff P, Darby D, Smith C, Woodward M, Merory J, Tochon-Danguy H, O'Keefe G, Klunk WE, Mathis CA, Price JC, Masters CL, Villemagne VL. Imaging beta-amyloid burden in aging and dementia. Neurology. 2007; 68:1718–1725. [PubMed: 17502554]
49. Price JC, Klunk WE, Lopresti BJ, Lu X, Hoge JA, Ziolko SK, Holt DP, Meltzer CC, Dekosky ST, Mathis CA. Kinetic modeling of amyloid binding in humans using PET imaging and Pittsburgh Compound-B. J Cereb Blood Flow Metab. 2005; 11:1528–1547. [PubMed: 15944649]
50. Buckner RL, Snyder AZ, Shannon BJ, LaRossa G, Sachs R, Fotenos AF, Sheline YI, Klunk WE, Mathis CA, Morris JC, Mintun MA. Molecular, structural, and functional characterization of Alzheimer's disease: evidence for a relationship between default activity, amyloid, and memory. J Neurosci. 2007; 25:7709–7717. [PubMed: 16120771]
51. Rabinovici GD, Furst AJ, O'Neil JP, Racine CA, Mormino EC, Baker SL, Chetty S, Patel P, Pagliaro TA, Klunk WE, Mathis CA, Rosen HJ, Miller BL, Jagust WJ. ^{11}C-PIB PET imaging in Alzheimer disease and frontotemporal lobar degeneration. Neurology. 2007; 68:1205–1212. [PubMed: 17420404]
52. Engler H, Santillo AF, Wang SX, Lindau M, Savitcheva I, Nordberg A, Lannfelt L, Langstrom B, Kilander L. In vivo amyloid imaging with PET in frontotemporal dementia. Eur J Nucl Med Mol Imaging. 2007; 35:100–106. [PubMed: 17846768]
53. Drzezga A, Grimmer T, Henriksen G, Stangier I, Perneczky R, et al. Imaging of amyloid plaques ad cerebral glucose metabolism in semantic dementia and Alzheimer's disease. Neuroimage. 2007; 39:619–633. [PubMed: 17962045]

54. Gomperts SN, Rentz DM, Moran E, Becker JA, Locascio JJ, Klunk WE, Mathis CA, Elmaleh DR, Shoup T, Fischman AJ, Hyman BT, Growdon JH, Johnson KA. Imaging amyloid deposition in Lewy body diseases. Neurology. 2008; 71:903–910. [PubMed: 18794492]
55. Yi L, Rinne J, Mosconi L, et al. Regional analysis of FDG and PIB-PET images in normal aging, mild cognitive impairment, and Alzheimer's disease. Eur J Nucl Mel Mol Imaging. 2008; 35:2169–2181.
56. Roy CS, Sherrington CS. On the regulation of the blood supply of the brain. J Physiol. 1890; 11:85–108.
57. Sokoloff L. Relationships among local functional activity, energy metabolism, and blood flow in the central nervous system. Fed Proc. 1981; 40:2311–2316. [PubMed: 7238911]
58. Raichle ME, Mintun MA. Brain work and brain imaging. Annu Rev Neurosci. 2006; 29:449–476. [PubMed: 16776593]
59. Koeppe RA, Gilman S, Joshi A, Liu S, Little R, Junck L, Heumann M, Frey KA, Albin RL. [^{11}C]DTBZ and [^{18}F]FDG PET measures in differentiating dementias. J Nuc Med. 2005; 46:936–944.
60. McKhann G, Drachman D, Folstein M, et al. Clinical diagnosis of Alzheimer disease: report of NINCDS-ADRDAwork group under the auspices of Department of Health and Human Services Task Force on Alzheimer's disease. Neurology. 1984; 34:939–944. [PubMed: 6610841]
61. McKeith IG, Dickson DW, Lowe J, et al. Diagnosis and management of dementia with Lewy bodies: Third report of the DLB consortium. Neurology. 2005; 65:1863–1872. [PubMed: 16237129]
62. Neary D, Snowden JS, Gustafson L, et al. Frontotemporal lobar degeneration: A consensus on clinical diagnostic criteria. Neurology. 1998; 51:1546–1554. [PubMed: 9855500]
63. Petersen RC. Mild cognitive impairment as a diagnostic entity. J Intern Med. 2004; 256:183–194. [PubMed: 15324362]
64. Koeppe RA, Frey KA, Kume A, Albin R, Kilbourn MR, Kuhl DE. Equilibrium versus compartmental analysis for assessment of the vesicular monoamine transporter using (+)-alpha-[11C]dihydrotetrabenazine (DTBZ) and positron emission tomography. J Cereb Blood Flow Metab. 1997; 17:919–931. [PubMed: 9307605]
65. Talariach, J.; Tournoux, P. Co-Planar Stereotaxic Atlas of the Human Brain: 3-D Proportional System—An Approach to Cerebral Imaging. New York, NY: Thieme Medical Publishers; 1988.
66. Minoshima S, Koeppe RA, Frey KA, Kuhl DE. Anatomic standardization: linear scaling and nonlinear warping of functional brain images. J Nucl Med. 1994; 35:1528–1537. [PubMed: 8071705]
67. Minoshima S, Frey KA, Foster NL, Kuhl DE. Preserved pontine glucose metabolism in Alzheimer disease: a reference region for functional brain image (PET) analysis. J Comput Assist Tomogr. 1995; 19:541–547. [PubMed: 7622680]
68. Minoshima S, Frey KA, Koeppe RA, Foster NL, Kuhl DE. A diagnostic approach in Alzheimer's disease using three-dimensional stereotactic surface projections of fluorine-18-FDG PET. J Nucl Med. 1995; 36:1238–1248. [PubMed: 7790950]
69. Jagust W, Reed B, Mungas D, Ellis W, Decarli C. What does fluorodeoxyglucose PET imaging add to a clinical diagnosis of dementia? Neurology. 2007; 69:871–877. [PubMed: 17724289]
70. Silverman DHS. Brain 18F-FDG PET in the diagnosis of neurodegenerative dementias: comparison with perfusion SPECT and with clinical evaluations lacking nuclear imaging. J Nucl Med. 2004:594–607. [PubMed: 15073255]
71. Silverman DH, Gambhir SS, Huang HW, Schwimmer J, Kim S, Small GW, Chodosh J, Czernin J, Phelps ME. Evaluating early dementia with and without assessment of regional cerebral metabolism by PET: a comparison of predicted costs and benefits. J Nucl Med. 2002:253–266. [PubMed: 11850493]
72. Mosconi L, Tsui WH, Herholz K, et al. Multicenter, standardized ^{18}F-FDG PET diagnosis of mild cognitive impairment, Alzheimer's disease, and other dementias. J Nucl Med. 2008; 49:390–398. [PubMed: 18287270]

73. Hoffman JM, Welsh-Bohmer KA, Hanson M, Crain B, Hulette C, Earl N, Coleman RE. FDG PET imaging in patients with pathologically verified dementia. J Nucl Med. 2000; 41:1920–1928. [PubMed: 11079505]

74. McKeith IG, Ballard CG, Perry RH, Ince PG, O'Brien JT, Neill D, et al. Prospective validation of consensus criteria for the diagnosis of dementia with Lewy bodies. Neurology. 2000; 54:1050–1058. [PubMed: 10720273]

75. Alladi S, Xuereb J, Bak T, Nestor P, Knibb J, Patterson K, Hodges JR. Focal cortical presentations of Alzheimer's disease. Brain. 2007; 130:2636–2645. [PubMed: 17898010]

76. Rabinovici GD, Jagust WJ, Furst AJ, Ogar JM, Racine CA, et al. Aβ amyloid and glucose metabolism in three variants of primary progressive aphasia. Ann Neurol. 2008; 64:388–401. [PubMed: 18991338]

77. Rabinovici GD, Furst AJ, O'Neil JP, Racine CA, Mormino EC, Baker SL, Chetty S, Patel P, Pagliaro TA, Klunk WE, Mathis CA, Rosen HJ, Miller BL, Jagust WJ. 11C-PIB PET imaging in Alzheimer disease and frontotemporal lobar degeneration. Neurology. 2007; 68:1205–1212. [PubMed: 17420404]

78. Rinne JO, Laine M, Kaasinen V, Norvasuo-Heilä MK, Någren K, Helenius H. Striatal dopamine transporter and extrapyramidal symptoms in frontotemporal dementia. Neurology. 2002; 58:1489–1493. [PubMed: 12034784]

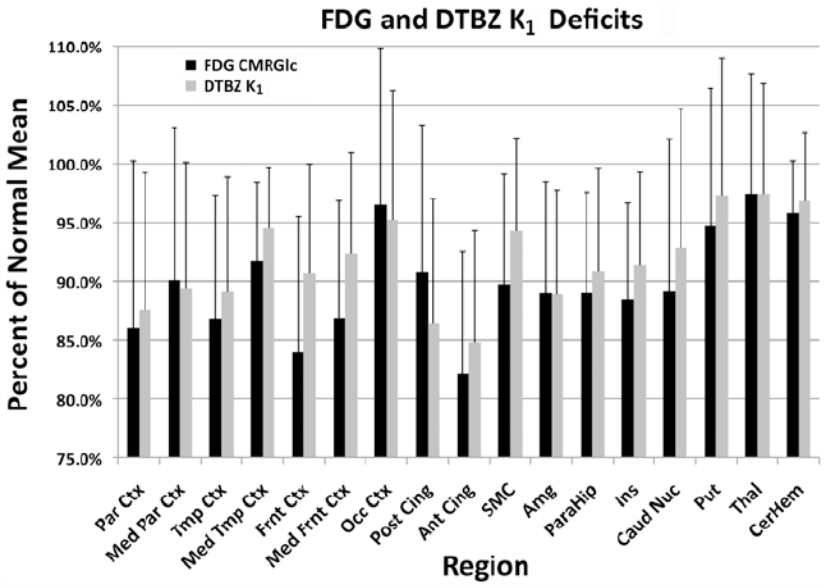

Figure 1. Regional Metabolic and Perfusion Deficits

Bar graphs of regional metabolic and perfusion deficits, expressed as percent of control mean, for 50 subjects with dementia or MCI. Magnitudes of the deficits observed by either FDG CMR_{glc} or DTBZ K_1 vary similarly across regions. Error bars represent 1 standard deviation of the percent of normal mean for all patient subjects.

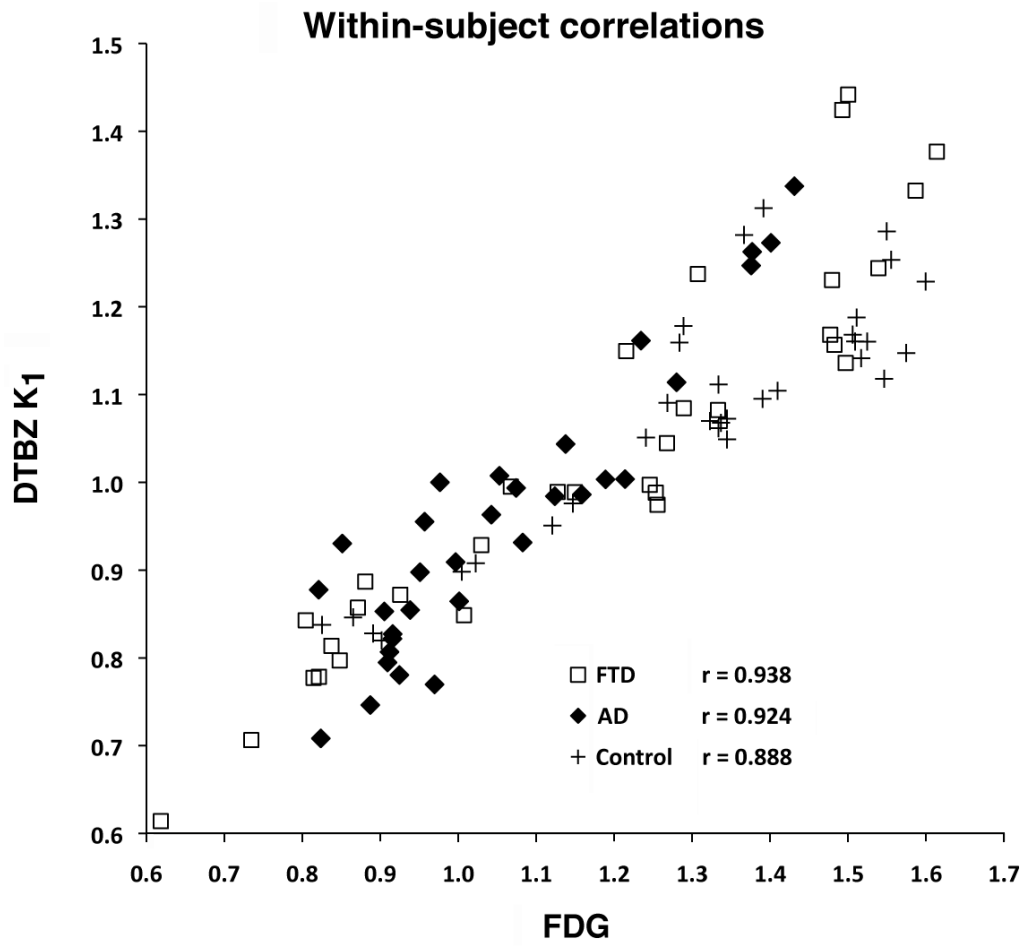

Figure 2. Within-Subjects Correlations

Representative within-subjects correlations (across the 34 regions examined) between FDG and DTBZ K_1 for an individual subject with AD, one with FTD, and one control subject. FDG and DTBZ K_1 values are each normalized to the average of pons and cerebellar vermis. Each data point represents the normalized K_1 and FDG values for one of the 34 regions.

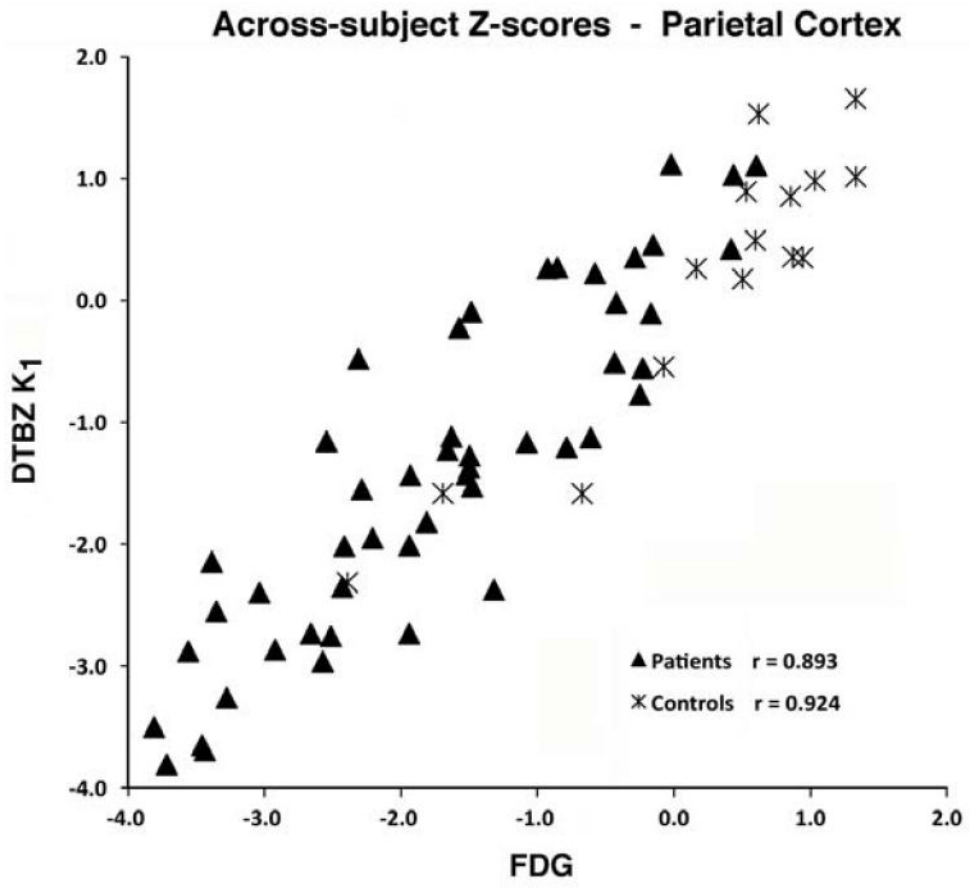

Figure 3. Across-Subject Correlations of Z-scores for Parietal Cortex

Across-subject correlations of Z-scores between FDG CMR_{glc} and DTBZ K_1 in the parietal cortex for patients (all demented and MCI subjects) and for control subjects. Each data point represents the Z-scores from normalized K_1 and FDG values for a single subject.

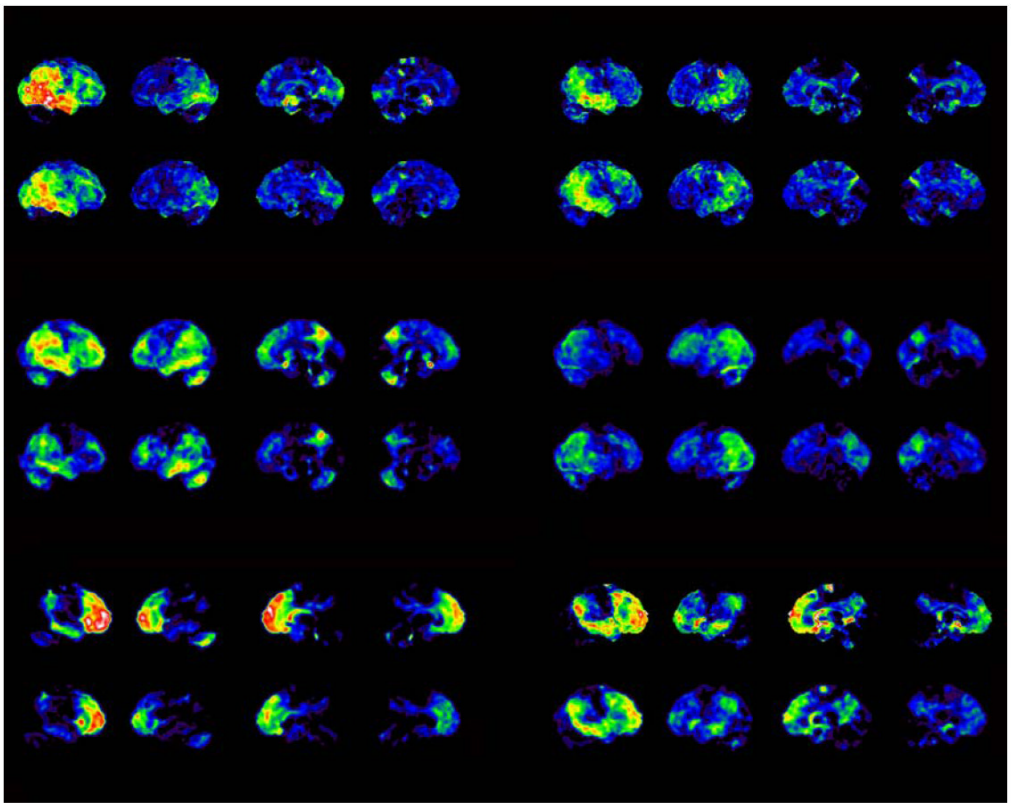

Figure 4. SSP Projection Images

SSP projection images of Z-scores of FDG CMR_{glc} and DTBZ K_1 deviations relative to control datasets for six representative patient subjects. The four surface projections from left to right for each of the subjects represent right lateral, left lateral, right medial, and left medial views. Each data set is scaled to show a range of deficits from 0.0 to 5.0 (standard deviations below control mean). The patterns of deviation from normal are markedly similar.

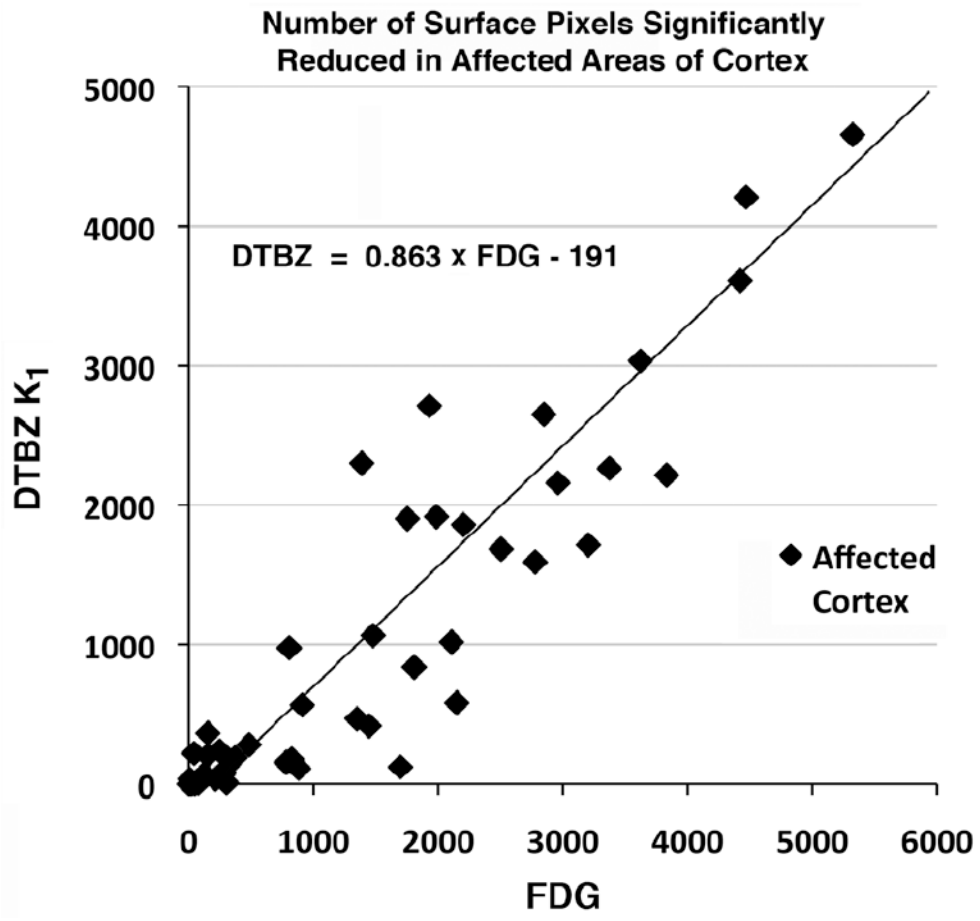

Figure 5. Extent of Deficits Affected Cortex

Number of SSP surface map pixels in affected cortex with greater than a 2.5 standard deviation decrease from normal control. Each point on the plot represents one of the 50 patient subjects. (see Supplementary Fig. 2 for description of affected cortex.)